Control Strategy for a Multilevel Inverter in Grid-Connected Photovoltaic Applications

Gabriele Grandi, Darko Ostojic, Claudio Rossi, Alberto Lega
Dipartimento di Ingegneria Elettrica
Alma Mater Studiorum - Università di Bologna
Viale Risorgimento, 2 – 40136, Bologna (Italy)
[*firstname.lastname*]@mail.ing.unibo.it

***Abstract*—A novel conversion structure for photovoltaic (PV) grid connection is proposed in this paper. The conversion system is aimed to be relatively simple and effective in medium and high power range. The topology utilizes a dual two-level voltage source inverter (VSI), fed by two insulated PV fields, supplying a grid transformer with open-end connection. Use of proposed scheme doubles the output power range of the conversion system with respect to the rated power of a single inverter, without the need of series/parallel connections of power switches. Furthermore, the dual inverter structure allows multilevel voltage waveforms, reducing grid current harmonics and mitigating output voltage derivatives.**

An original control method has been introduced to regulate the dc-link voltages for each VSI. The proposed algorithm has been verified by numerical tests with reference to different operating conditions.

I. INTRODUCTION

Distributed power generation systems are widely recognized as an unpreventable trend in today's power utilities. Among them, use of photovoltaic (PV) solar energy for grid-connected application is fast growing market. Since the PV technology has some insuperable features, such are noiseless, fuel- and pollution-free generation, lack of wearing parts and high reliability, it has potential to become main renewable energy source of the future. In an effort to diminish shortcomings such as high initial installation cost and low energy conversion efficiency, many power converter configurations and maximum power point (MPP) control algorithms had been proposed [1]-[2].

In spite of vast number of proposed PV-to-grid converter topologies, including complex multistage converters, high-power photovoltaic systems (starting from few kW) are dominated by the simplest topology with standard three-phase (or even single-phase) inverter and line-frequency transformer. Namely, it has been demonstrated that use a lower amount of panels connected in series improves the global efficiency of the PV generator as a result of a reduction in cell production mismatch, partial shadows of the array, etc. The parallel connection of the cells solves the "weakest-link" problem, but the voltage at output is low (few tens of volts) and requires application of the transformer (or dc-dc converter). The transformer also provides standards compliance regarding limits on the dc current injection into the grid and galvanic insulation requirements between PV panels and the grid.

In order to reduce current and voltage harmonics on the ac side and to increase the power rating of the conversion system, multilevel inverter topologies were proposed for PV applications, since it is easy to obtain more than one dc supply [3-5]. However, their application implies complex layout (additional switches, diodes and/or capacitors) and control. In these multilevel topologies it is difficult to manage imbalance loading of the different PV strings and consequently is difficult to achieve MPP from each individual string.

A novel topology for PV grid-connected systems is proposed in this paper (Fig.1). It utilizes a dual two-level converter structure [6] connected to open-end primary windings of a standard three-phase transformer. Each inverter can be directly coupled with the panels, or through dc/dc stage (dashed lines in Fig. 1). The secondary windings of the transformer are directly connected to the grid. Note that the coupling inductor which is necessary for the grid connection of a VSI can be given by the leakage inductance of the transformer.

Use of this power stage scheme doubles the output power range of the conversion system with respect to the rated power of a single inverter [7], without the need of series/parallel connections of power switches. Furthermore, the dual inverter system acts as a multilevel converter, provided that a proper switching technique is adopted [8], with considerable improvements of the output voltage waveforms.

This converter topology requires two separate dc sources in order to avoid circulation of common-mode dc current, maximizing the output voltage [6]. These requirements can be

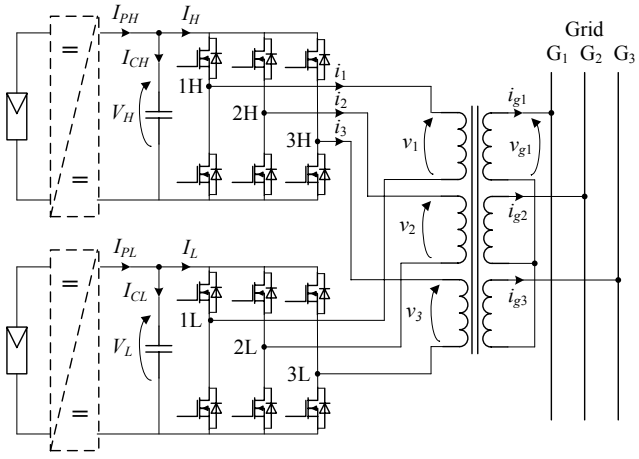

Fig. 1. Scheme of the proposed dual-inverter configuration.

easily fulfilled in the case of PV panels, because it is easy and convenient to separate the whole PV field in two sub-fields.

The switching technique adopted for the dual inverter is able to regulate the power sharing from two dc sources inside each switching cycle. This technique was introduced in the past for battery-powered systems in motor drive application [7], [8] and is now proposed for a dual supply PV system.

A typical configuration for this conversion system is based on parallel connection of PV panels for each sub-field. The resulting PV field voltage is generally between 30-50 V, which allows use of low-voltage MOSFETs. These types of MOSFETs are widely used in automotive applications and they are very cheap semiconductor devices. Furthermore those components have good efficiency, since their on-state resistance is a strong decreasing function of the blocking voltage rating. However, maximum power rating of converter using low PV field voltage is limited to few tens of kW. For higher powers the proposed topology can be utilized with higher dc side inverter voltage (400-700 V). Demanded dc voltage range can be directly obtained by increased PV field voltage with series connection of more panels. Another possibility is inclusion of intermediate dc/dc converters, which simultaneously take over role of MPP trackers, enabling optimal and constant dc bus voltages for the dual inverter. For even higher powers (above few hundred kW) the converter can be connected to medium voltage grid (10-20 kV) through a coupling transformer with a proper turn ratio.

II. Principle of Operation

The proposed system is symmetric, having both inverters with equal ratings and two equal groups of panels supplying them. Nevertheless two distinct voltage controllers have to be implemented to compensate unavoidable mismatches, originating from cell production nonidealities or small differences in cleanness and solar irradiance. In the following, the converter voltage control is described in more detail, while the MPP and other necessary supervisory tasks of the system control are not discussed further.

Fig. 2 shows the basic control scheme of the converter, which is based on two control tasks. A primary control task is the voltage regulation of PV sub-fields in order to accomplish MPP for both of them. A second control task is the injection of the PV power into the grid, by using a dual two-level converter connected at the open-end primary windings of a three-phase transformer. By synthesizing different output voltages for the two VSIs is possible to supply different powers from the two PV sub-fields to the grid.

The two dc voltages (V_H, V_L) are controlled by two PI controllers, having as input, the reference voltage (V_H^*, V_L^*) of the two panels coming from the MPP algorithm and giving as output the reference of two dc currents (I^*_H, I^*_L). A feed-forward action can be added in order to compensate sudden changes in PV currents (I_{PH}, I_{PL}). Its utilization depends on the availability of the current transducer and on the required response dynamic.

By neglecting inverter and transformer losses and assuming pure sinusoidal quantities for the ac side of the converter, the power balance equation in steady-state between the two dc sides and the grid side of the converter is

$$V_H I_H + V_L I_L = \frac{3}{2} V \frac{N_2}{N_1} I_g \tag{1}$$

where V is the amplitude of inverter output phase voltage applied to a primary winding of the coupling transformer with winding ratio N_1/N_2 and I_g is the magnitude of the current injected into the grid.

By using the power balance equation (1) the reference of the magnitude of the current injected into the grid is

$$I_g^* = \frac{2}{3} \frac{N_1}{N_2} \frac{V_H I_H^* + V_L I_L^*}{V}. \tag{2}$$

From this point, the control of the converter is realized by introducing the space vector representation of three phase quantities. A reference unity voltage vector $\hat{v}_g$ in phase with the fundamental grid voltage component is generated by using a synchronization system [9]. Multiplying $\hat{v}_g$ by the reference grid current I_g^* calculated in (2), the reference vector $\bar{i}_g^*$ of

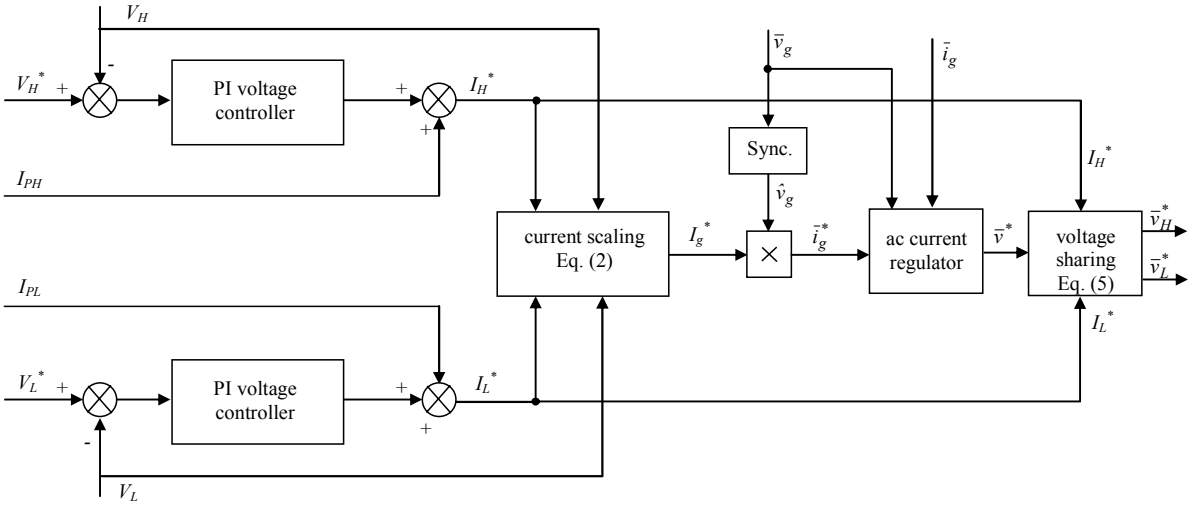

Fig. 2. Block diagram of proposed control system.

the current injected into the grid is generated. In this way the grid current is in phase with the fundamental component of the grid voltage and the system directly controls the active power injected into the grid. If it is required, reactive or harmonic compensation current references can be added in as many ways as shown in [10].

The control of the grid current is performed by using a regulator acting on the current through the leakage reactance of the coupling transformer. Among the possible choices, the use of two PI regulators, implemented on the two axis of a rotating frame synchronous with the grid fundamental voltage, are usually preferred for the good trade-off between simplicity and performance.

The output variable of the grid current regulator is the inverter output voltage reference $\bar{v}^*$ that is applied at the primary windings of the transformer. Output voltage reference $\bar{v}^*$ is given by summing the two reference voltages $\bar{v}_H^*, \bar{v}_L^*$ generated by the two sides of the multilevel converter

$$\bar{v}^* = \bar{v}_H^* + \bar{v}_L^* . \tag{3}$$

Being the inverter output current $\bar{i}$ the same for the two inverter sides and assuming $\bar{v}_H^*$ and $\bar{v}_L^*$ lying in the same direction, the two ratios $\bar{v}_H^* / \bar{v}^*$ and $\bar{v}_L^* / \bar{v}^*$ represent the sharing of the total power supplied to the grid by the two inverter and then by the two dc sources.

The power balance equation (2) can be rewritten for the two inverters side as

$$\frac{\bar{v}_H^*}{\bar{v}^*} = \frac{V_H I_H^*}{V_H I_H^* + V_L I_L^*} = k \quad , \quad \frac{\bar{v}_L^*}{\bar{v}^*} = \frac{V_L I_L^*}{V_H I_H^* + V_L I_L^*} = 1 - k . \tag{4}$$

In the case the two panels have similar working condition, it can be assumed that $V_H \cong V_L$, and (4) can be further simplified yielding to the following equations for the two inverters reference output voltages $\bar{v}_H^*$, $\bar{v}_L^*$

$$\bar{v}_H^* \cong \frac{I_H^*}{I_H^* + I_L^*} \bar{v}^* , \quad \bar{v}_L^* \cong \frac{I_L^*}{I_H^* + I_L^*} \bar{v}^* . \tag{5}$$

These two voltages will be then synthesized at each switching cycle by using the modulation technique presented in [8] and briefly described in Section III. In this converter, owing to the dual two level converter characteristics, the inverter reference output voltages $\bar{v}_H^*$, $\bar{v}_L^*$ are also subject to a limitation depending on the dc voltage and the modulation index. The admitted range of voltage $\bar{v}_H^*$ and $\bar{v}_L^*$ will be shown in the next Section.

III. Multilevel Operation

With reference to the scheme of Fig. 1, and assuming $V_H = V_L = E$, the voltage vectors $\bar{v}_H$ and $\bar{v}_L$ generated by the converter are given by 18 different output active voltage vectors and one null vector, as represented by the red dots in Fig. 3. By using the SVM technique, these 19 voltage vectors can be modulated to obtain any output voltage vector lying inside the outer hexagon, having a side length of 4/3 E. In particular, with reference to sinusoidal steady state operating conditions, the maximum magnitude of the output voltage vector $\bar{v}^*$, that can be generated by the converter, is $2/\sqrt{3}\ E$ (i.e., the radius of the inscribed circle).

A correct multilevel operation requires the output voltage vector $\bar{v}^*$ to be synthesized by modulating three voltage vectors $\bar{v}_a, \bar{v}_b, \bar{v}_c$, corresponding to the vertices of the triangle in which the output voltage vector $\bar{v}^*$ is located.

The output voltage $\bar{v}^*$ can be expressed by means of the duty cycles a,b,c of the three adjacent main vectors as follows:

$$\bar{v}^* = a\,\bar{v}_a + b\,\bar{v}_b + c\,\bar{v}_c , \tag{6}$$

where the duty-cycles a,b,c are given by standard SVM equations.

According to the assumption made in (4), the inverter voltage vectors $\bar{v}_H^*$ and $\bar{v}_L^*$ are in phase and lay in the same sector, as represented in Fig. 4. This assumption allows the two inverters to synthesize $\bar{v}_H^*$ and $\bar{v}_L^*$ by modulating the same adjacent active vectors $\bar{v}_\alpha, \bar{v}_\beta$. As a consequence, the resulting output voltage vectors of the two inverters are:

$$\begin{cases} \bar{v}_H^* = \alpha_H\,\bar{v}_\alpha + \beta_H\,\bar{v}_\beta + \gamma_H\,\bar{0} \\ \bar{v}_L^* = \alpha_L\,\bar{v}_\alpha + \beta_L\,\bar{v}_\beta + \gamma_L\,\bar{0} \end{cases} . \tag{7}$$

In (7) $\alpha_H, \beta_H, \gamma_H$ are the duty cycles of active vectors $\bar{v}_\alpha, \bar{v}_\beta$ and null vector for the inverter H, respectively. In the same way, $\alpha_L, \beta_L, \gamma_L$ are the duty cycles of active vectors $\bar{v}_\alpha, \bar{v}_\beta$, and null vector for the inverter L, respectively.

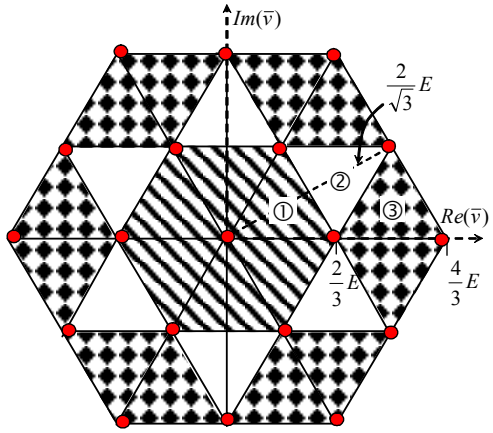

Fig. 3. Highlight of the triangles in the three different regions ①, ②, and ③.

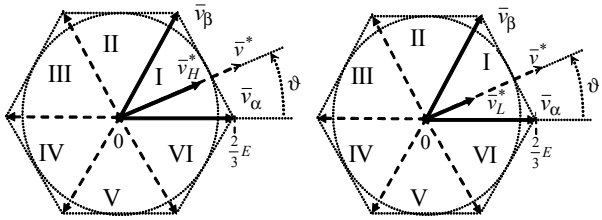

Fig. 4. Reference voltage vectors $\bar{v}_H$ and $\bar{v}_L$ generated by using the same two adjacent active vectors $\bar{v}_\alpha$, $\bar{v}_\beta$.

Once the duty cycle of the two inverters have been calculated a proper switching sequence must be defined.

The main requirements of the switching sequence are the minimization of the number of switch commutations and the application of correct voltage vectors during commutations. In [8] it has been defined a switching sequence complying with these requirement that can be conveniently used for this application.

The constraints on the duty-cycles of the two inverters, $0 \le \alpha_L, \beta_L, \gamma_L \le 1$ and $0 \le \alpha_L, \beta_L, \gamma_L \le 1$, introduce a limit in the range of variation of the power sharing coefficient *k*. In particular, the range of variation of *k* can be expressed as a function of the desired output vector $\bar{v}^*$.

Assuming sinusoidal output voltages $\left(\bar{v}^* = V^* e^{j\vartheta}\right)$ and introducing the modulation index

$$m = V^* \Big/ \frac{2}{\sqrt{3}} E \qquad (0 \le m \le 1) \tag{8}$$

the admitted values of *k* are given by

$$\frac{1}{2} - a \le k \le \frac{1}{2} + a, \tag{9}$$

where,

$$a = \frac{1-m}{2m}. \tag{10}$$

By means of (9) and (10) the possible values of *k* can be determined as function of the modulation index *m*. This relationship is graphically represented in Fig. 5. The dashed area defines the possible values of *k* and then determines to which extent the power sharing between the two inverters can be changed. By analyzing Fig. 5 the following considerations can be made.

- If the maximum output voltage is required (i.e. *m* = 1), it is not possible to regulate the power sharing between the two dc sources. In this case only the value $k = 0.5$ is acceptable and the two sources generate the same voltages and supply the same power to the grid.
- For $0.5 \le m \le 1$ the coefficient *k* is limited as function of *m*, showing a decreasing range of variation as *m* increases.

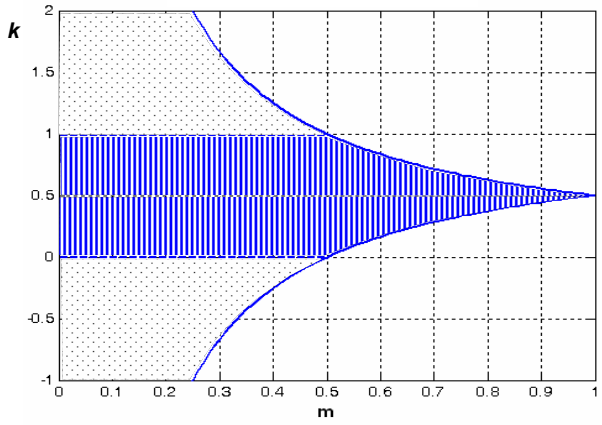

Fig. 5. Limits of power sharing coefficient *k* vs. modulation index *m*.

- For $m < 0.5$ the output voltage vector lies within the circle of radius $E/\sqrt{3}$. In this case, the output power can be supplied by the two inverters with any ratio. In particular, if *k* is set to 0, all the load power is supplied by inverter *L*, whereas if *k* is set to 1 all the load power is supplied by inverter *H*. This is a very important feature of this converter since it is possible to inject power to the grid load by using one inverter only, if necessary.

It should be considered that in ordinary operating condition the two inverters supply similar values of power and then the parameter *k* will be very close to 0.5.

IV. Simulation Results

The simulation model of the proposed topology and control scheme represented in Figs. 1 and 2 was implemented in MATLAB-Simulink, using *SimPowerSystems* library. The component ratings used for model are based on real laboratory equipment which will be used for future experimental tests. The PV panels have been electrically represented by the fitted I-V characteristic of a parallel arrangement of "*Solar Shell*" SP150 modules. The main characteristics of the PV generation system are summarized in Table I.

TABLE I
System Prototype Characteristics

Quantity	*Value*		*Quantity*	*Value*
PV panel power (peak)	150 W		Line-to-line grid voltage	400 V, 50 Hz
PV field power (peak)	1.2 kW		Transformer rated power	1.5 kVA
PV sub-field connection (2 sub-fields)	4 in parallel		Transformer short-circuit voltage	5.6 %
PV sub-filed short-circuit current	20 A		dc-link capacitance	2 mF
PV sub-field open-circuit voltage	45 V		PWM carrier frequency	20 kHz

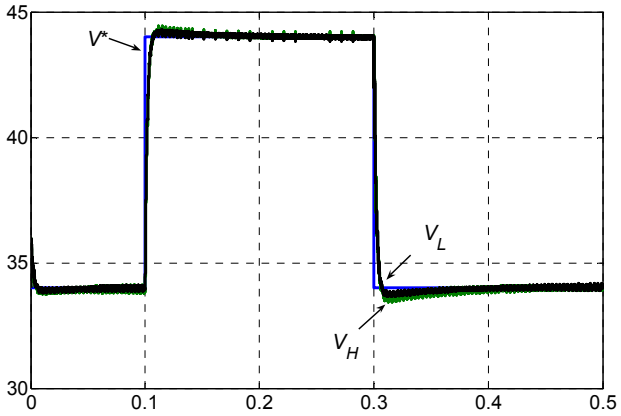

Fig. 6. Inverters dc voltage response for the case of step change in voltage reference.

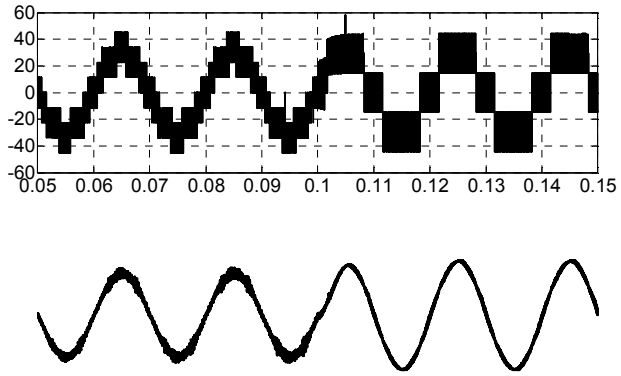

Fig. 7. Phase voltage and current applied to the primary winding of the transformer by the dual two-level converter.

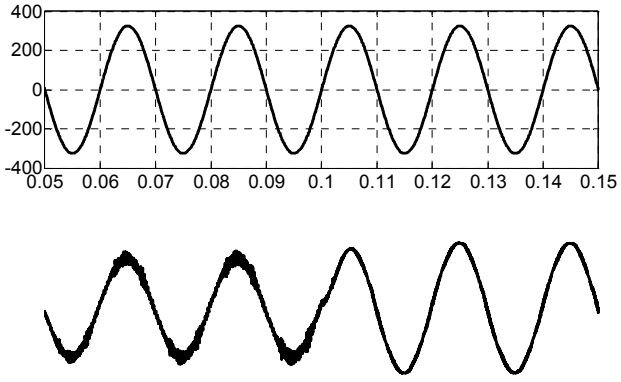

Fig. 8. Grid phase voltage and grid injected current.

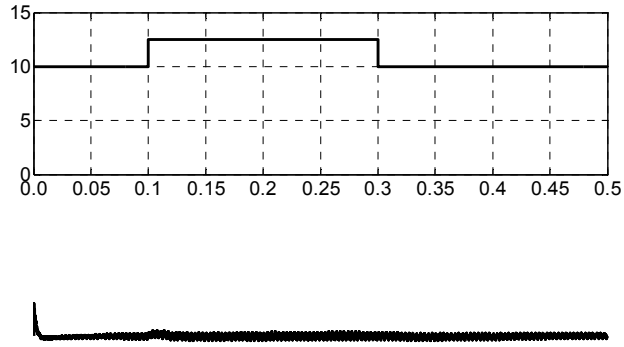

Fig. 9. Inverters dc voltage in the case of step change of the injected dc current.

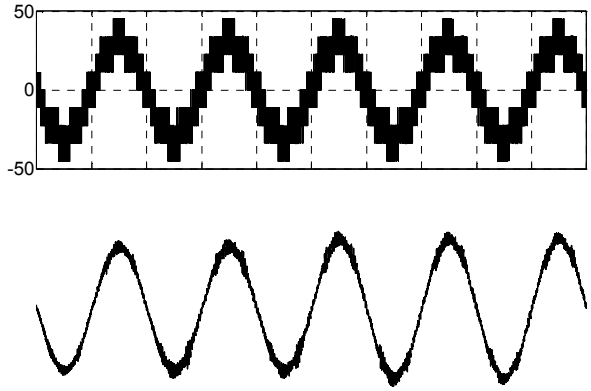

Fig. 10. Phase voltage and current applied to the primary winding of the transformer by the dual two-level converter.

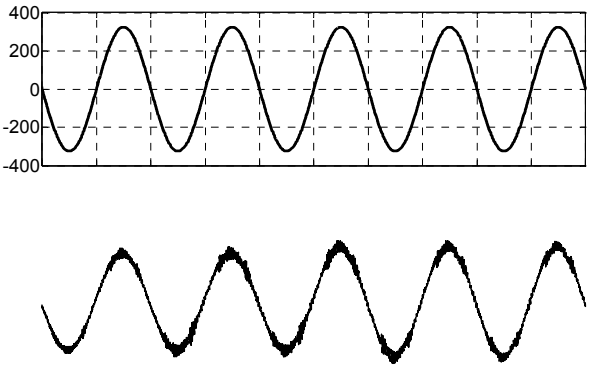

Fig. 11. Grid phase voltage and grid injected current.

In simulation tests reference is made to the system topology shown in Fig. 1 with a direct connection between the two PV sub-fields and the two inverters. In this case the MPPT regulation is achieved by the change of inverters' dc bus voltage. Figures 6-8 show the time behavior of the inverter in case of sudden change of voltage reference, demanded by the MPPT control algorithm as a response to the change of solar irradiation. In particular, Fig. 6 shows very fast and almost identical response for both voltages. The output of the dual inverter during the whole executed simulation has been shown in the zoomed view of Fig. 7. The current is very slightly lagging the voltage because of the leakage inductors and transformer reactive power demand. The figure also shows that converter modulation corresponds to a proper

multilevel operation since commutations among adjacent voltage levels are always obtained. Noticeably after the rise of available dc voltage number of used voltage levels decreases because inverter's output voltage transfers to the inner hexagon. The grid current and voltage are in phase, and current ripple is acceptable as shown in Fig. 8.

Another set of simulations is given for the topology with dc/dc converter stage between the PV sub-fields and the inverters Fig. 1. Figure 9-11 show the response of the system to a sudden change in value of injected dc current. The response of control system is very fast and therefore almost without noticeable change in dc voltage as shown in Fig.9b. In Fig. 10 is shown a zoomed view of an output voltage of the converter and of the corresponding transformer input current. In Fig. 11 is shown a zoomed view of a phase to neutral grid voltage and of the corresponding phase current injected into the grid. These two last figures verify the capability of the converter to operate correctly during severe transients of the input power.

VI. CONCLUSION

A novel conversion topology for the grid connection of a photovoltaic generation system is presented and discussed in this paper. The proposed power conditioner utilizes a multilevel converter named dual two-level converter. The topology is based on a power stage composed by two standard two level converter and includes two insulated PV sub-fields and a three-phase open-winding transformer. A control algorithm is introduced for the system regulation. It is able to provide power generation with unity power factor and maximum power point tracking, even in case of two unbalanced subfields. Numerical simulations carried out in different operating conditions show good performance of the proposed control algorithm, confirming the effectiveness of the whole conversion topology.

REFERENCES

[1] S. Kjaer, J. Pedersen, F. Blaabjerg: "A Review of Single-Phase Grid-Connected Inverters for Photovoltaic Modules," IEEE Trans. on Industrial Applications, vol. 41, No. 5, Sep 2005, pp. 1292-1306.

[2] T. Shimizu, M. Hirakata, T. Kamezawa, and H. Watanabe, "Generation control circuit for photovoltaic modules," IEEE Trans. on Power Electronics, vol. 16, No. 3, May 2001, pp. 293-300.

[3] S. Alepuz, S. Busquets-Monge, J. Bordonau, J. Gago, D. Gonzalez, J. Balcells, "Interfacing Renewable Energy Sources to the Utility Grid Using a Three-Level Inverter," IEEE Trans. on Industrial Electronics, vol. 53, no. 5, Oct. 2006, pp. 1504-1511.

[4] Y. Kawabata, N. Yahata, M. Horii, E. Ejiogu, T. Kawabata, "SVG using open-winding transformer and two inverters," Proc. of IEEE Power Electronics Spec. Conf., PESC 2004., vol.4, pp. 3039- 3044.

[5] K. Corzine, A. S. Sudhoff, C. Whitcomb, "Performance characteristics of a cascaded two-level converter," IEEE Trans. on Energy Conversion, vol. 14, No. 3, Sept. 1999, pp. 433-439.

[6] M. Baiju, K. Mohapatra, R. Kanchan, K. Gopakumar, "A dual two-level inverter scheme with common mode voltage elimination for an induction motor drive," IEEE Trans. on Power Electronics vol. 19, No. 3, May 2004, pp. 794-805.

[7] G. Grandi, C. Rossi, A. Lega, D. Casadei, "Power balancing of a multilevel converter with two insulated supplies for three-phase six-wire loads," Proc. of 11th European Conference on Power Electronics and Applications, EPE 2005, Dresden (D), September 11-14, 2005.

[8] G. Grandi, C. Rossi, A. Lega, D. Casadei, "Switching Technique for Dual-Two level Inverter Supplied by Two Separate Sources," Proc. of IEEE-APEC Anaheim (CA) (USA), Feb. 25 - Mar. 1, 2007.

[9] S. K. Chung, "A Phase Tracking System for Three Phase Utility Interface Inverters," IEEE Transaction on Power Electronics, vol. 15 no. 3, May 2000, pp. 431-438

[10] L.A. Moran, J.W. Dixon, R.R. Wallace, "A three- phase active power filter operating with fixed switching frequency for reactive power and current harmonic compensation," IEEE Trans. on Industrial Electronics, vol. 42, No. 4, 1996, pp. 402-408.